FEBS Letters 504 (2001) 126–132 FEBS 25152

Minireview

Insights from the structure of the yeast cytochrome bc_1 complex: crystallization of membrane proteins with antibody fragments

Carola Hunte*

Max-Planck-Institut für Biophysik, Abteilung Molekulare Membranbiologie, Heinrich-Hoffmann-Straße 7, D-60528 Frankfurt am Main, Germany

Received 11 July 2001; accepted 23 July 2001

First published online 6 August 2001

Edited by Andreas Engel and Giorgio Semenza

Abstract The ubiquinol:cytochrome *c* oxidoreductase (EC 1.20.2.2, QCR or cytochrome bc_1 complex) is a component of respiratory and photosynthetic electron transfer chains in mitochondria and bacteria. The complex transfers electrons from quinol to cytochrome *c*. Electron transfer is coupled to proton translocation across the lipid bilayer, thereby generating an electrochemical proton gradient, which conserves the free energy of the redox reaction. The yeast complex was crystallized with antibody Fv fragments, a promising technique to obtain well-ordered crystals from membrane proteins. The high-resolution structure of the yeast protein reveals details of the catalytic sites of the complex, which are important for electron and proton transfer.

Key words: Oxidoreductase; Complex III; Antibody fragment; Crystallization; Q cycle; Quinol

1. Introduction

Ubiquinol:cytochrome *c* oxidoreductase (QCR) belongs to a large family of cytochrome *bc* complexes, which are integral membrane proteins that serve as central components of the energy conversion machinery of photosynthesis and respiration in chloroplasts, mitochondria, and bacteria [1,2]. These multisubunit complexes couple electron transfer reactions to proton translocation across a membrane and thereby conserve the free energy of the redox reactions in an electrochemical proton gradient. The latter is utilized to drive energy-dependent processes like ATP synthesis or secondary transport.

Mitochondrial QCR catalyses electron transfer from ubiquinol to cytochrome *c* (CYC).

$$QH_2 + 2CYC(Fe^{3+}) + 2H_i^+ \rightarrow Q + 2CYC(Fe^{2+}) + 4H_o^+$$

The quinol mediated energy conversion is depicted in Fig. 1. Ubiquinol (QH_2) oxidation takes place at the Q_o site and involves a bifurcated electron transfer. One electron is transferred via the Fe_2S_2 iron–sulfur centre to haem c_1, the electron donor for cytochrome *c* reduction. The second electron is used to reduce ubiquinone (Q) bound at the Q_i site, thereby generating a relatively stable semiquinone. The latter is fully reduced to quinol after oxidation of a second quinol molecule at the Q_o site. Protons are taken up from the matrix side upon quinone reduction and released to the intermembrane space during quinol oxidation. The hydrophobic substrates quinol and quinone can freely diffuse within the phospholipid bilayer. This mechanism, known as Q cycle, facilitates proton translocation, thereby contributing to the generation of a proton gradient [3,4].

In the last few years, structures of vertebrate and yeast QCRs have become available [5–8], a breakthrough in understanding the enzyme mechanism and structure–function relationships. The 2.3 Å resolution structure of yeast QCR is the atomic structure of highest resolution available so far [8]. It allowed a detailed description of substrate- and inhibitor-binding sites, elucidating parts of the enzyme mechanism and suggesting pathways for proton transfer. Yeast QCR was crystallized with the help of antibody fragments. This approach appears to be of general importance for the crystallization of membrane proteins and will be outlined. In addition, some aspects of the structure–function relationship will be described here (for detailed reviews see [1–4,9]).

2. Crystallization of membrane proteins with antibody fragments

High-resolution structures of proteins provide valuable information to understand the mechanism of enzymes as well as for rational drug design. An excellent tool to obtain these structures is X-ray crystallography that requires well-ordered three-dimensional crystals as prerequisite. Three-dimensional crystallization of membrane proteins is hampered by the fact that these proteins have to be used in solubilized form. For this purpose their transmembrane portion, which in vivo resides in the phospholipid bilayer, is covered by a detergent micelle. Crystal formation is highly dependent on crystal contacts between surfaces of the hydrophilic protein domains, which are exposed to the bulk solvent [10–13]. In some families of membrane proteins, e.g. channels and transporters, the hydrophilic domains may be very small. A strategy to improve the likelihood of successful crystallization is to enlarge the hydrophilic surface of membrane proteins by surface expansion. This can be achieved by binding antibody fragments to the membrane protein, an approach that was successfully introduced by Michel and colleagues. They crystallized and determined the structure of the cytochrome *c* oxidase from *Paracoccus denitrificans* [14,15] and of a fragment of this protein

*Fax: (49)-69-96 76 94 23.
E-mail address: carola.hunte@mpibp-frankfurt.mpg.de (C. Hunte).

0014-5793/01/$20.00 © 2001 Published by Elsevier Science B.V. on behalf of the Federation of European Biochemical Societies.
PII: S0014-5793(01)02744-2

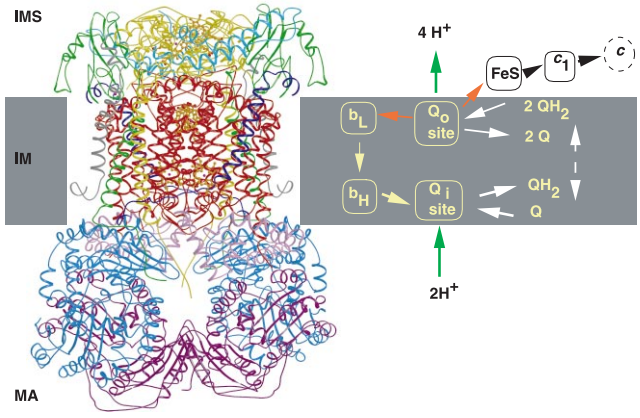

Fig. 1. Structural model of the dimeric yeast QCR and schematic representation of the Q cycle within a functional unit. Electron transfer from quinol to the acceptor cytochrome *c* is coupled to proton translocation. Electron transfer is indicated with white arrows, proton translocation in green. The bifurcated electron transfer upon quinol oxidation is highlighted in orange. The sites of quinol oxidation (Q_o site) and quinone reduction (Q_i site) are indicated. Cofactors are labelled as follows: FeS, Fe_2–S_2 cluster; b_L, haem b_L; b_H, haem b_H; c_1, haem c_1; *c*, haem *c*. Matrix, inner membrane and intermembrane space are indicated with MA, IM, IMS, respectively. The complex consists per monomer of nine subunits (represented as ribbon drawings), cytochrome *b* (red), Rieske protein (green), cytochrome c_1 (yellow) and their respective cofactors, the core proteins 1 (blue) and 2 (purple), and the small subunits QCR6 (cyan), QCR7 (faint purple), QCR8 (dark blue), and QCR9 (grey).

[16]. The structure of the yeast QCR was the third successful example for this technique [8].

Antibody fragments are well suited for this approach as they form a stable, rigid interaction with the antigen, thereby avoiding the introduction of flexible regions, which are in general an obstacle for crystallization. To ensure a stable associated 'domain', the selected antibody should not only bind to the native protein but should preferentially recognize a discontinuous epitope. A modification of the size of the domain is possible by using either Fv fragments (~28 kDa) or Fab fragments (~56 kDa). Furthermore, antibody fragments could be used to stabilize specific conformations of the protein to aid crystallization attempts. Three-dimensional crystallization of complex target antigens, such as viral flexible proteins, has been achieved with specifically bound Fab fragments [17]. Specifically tailored screening strategies are the key step in selecting suitable antibodies from hybridoma fusions or recombinant libraries. The introduction of an enzyme linked immunosorbent assay based on a nickel chelating matrix allows the presentation of native, detergent solubilized membrane protein via a histidine affinity tag. This method provided monoclonal antibodies exclusively against the native sodium/proton antiporter NhaA from *Escherichia coli* [18], a 12 transmembrane protein with very short solvent exposed loops. These antibodies were used to probe conformational changes of the antiporter upon regulatory pH shift [19].

Fab fragments produced by proteolytic digestion have been successfully used for crystallization [17]. Antibody fragments can be obtained by cloning the respective genes starting from hybridoma cell lines [20,21]. A variety of expression systems are used for the production of the fragments, including periplasmic expression in *E. coli* [20]. Alternatively, direct selection of recombinant antibody fragments from phage display libraries is well established [22,23] and a new approach to select antibodies from libraries evolved by ribosome display seems to be promising [24]. Recombinant fragments are versatile tools, providing for instance the introduction of fused affinity tags, so that they can be used for one-step purification of antigen–antibody complexes without the need to engineer the target protein [20].

Yeast QCR was crystallized with the help of an Fv fragment derived from the mAB_{18E11} [8]. The Fv fragment binds to the extrinsic domain of the iron–sulfur protein and provides generous space for the detergent micelle in the crystal packing (Fig. 2) [8]. It is found to be essential for the packing by mediating the crystal contacts.

3. Overall structure of QCR

The mitochondrial QCR is present as an intertwined homodimer (Figs. 1 and 2). In general, there is good overall homology of the vertebrate and yeast QCR structures. The centre of the complex is formed per monomer by eight transmembrane helices of cytochrome *b*, and attached to these central domain are the single transmembrane anchors of the Rieske protein and cytochrome c_1, the two other catalytic subunits. The extrinsic domains of the latter are located in the intermembrane space. On the same side of the membrane, QCR6 or the so-called hinge protein is bound. The homologue subunit of the bovine complex was shown to be important for cytochrome *c* binding [25]. Single transmembrane helices of subunits QCR8 and QCR9 are attached at the periphery of the catalytic core. In bovine QCR a third small, single transmembrane subunit is present [7]. It is a homologue of QCR10, a loosely associated subunit of the yeast complex, which is not present in the structure [8]. Interestingly, phospholipid molecules that are tightly bound within the transmembrane region are found in the structure of yeast QCR. Their well-defined binding sites suggest specific roles in assembly and function of the complex (Hunte et al., in prep.). The matrix portion of the complex is formed by two large subunits, COR1 and QCR2, the so-called core proteins, and by QCR7. The core proteins have high sequence similarity with soluble, matrix processing peptidases and are thought to be evolutionarily related to these Zn-binding proteases [26]. Core proteins do not have proteolytic activity in most species, with the exception of plants [26]. However, a biochemical study suggested residual proteolytic activity in bovine QCR [27]. Furthermore, the cleaved signal sequence of the Rieske protein is part of the bovine complex and is named subunit 11. The peptide is bound in a cleft between the core proteins and it has been speculated that the core proteins are active in processing the precursor [7]. Interestingly, structural comparison of bovine core protein 1 with the Zn-dependent protease thermolysin, which was performed by applying a reverse N-to-C orientation, demonstrated a striking similarity of the overall structural architecture and of the catalytic site of thermolysin and its proposed counterpart in the core protein, suggesting a structure–function convergence of these proteins [28] and supporting the close relation of core proteins with Zn-binding proteases.

4. Enzyme mechanism

The catalytic centre of the enzyme consists of cytochrome *b* with two non-covalently attached haem *b* groups, the Rieske

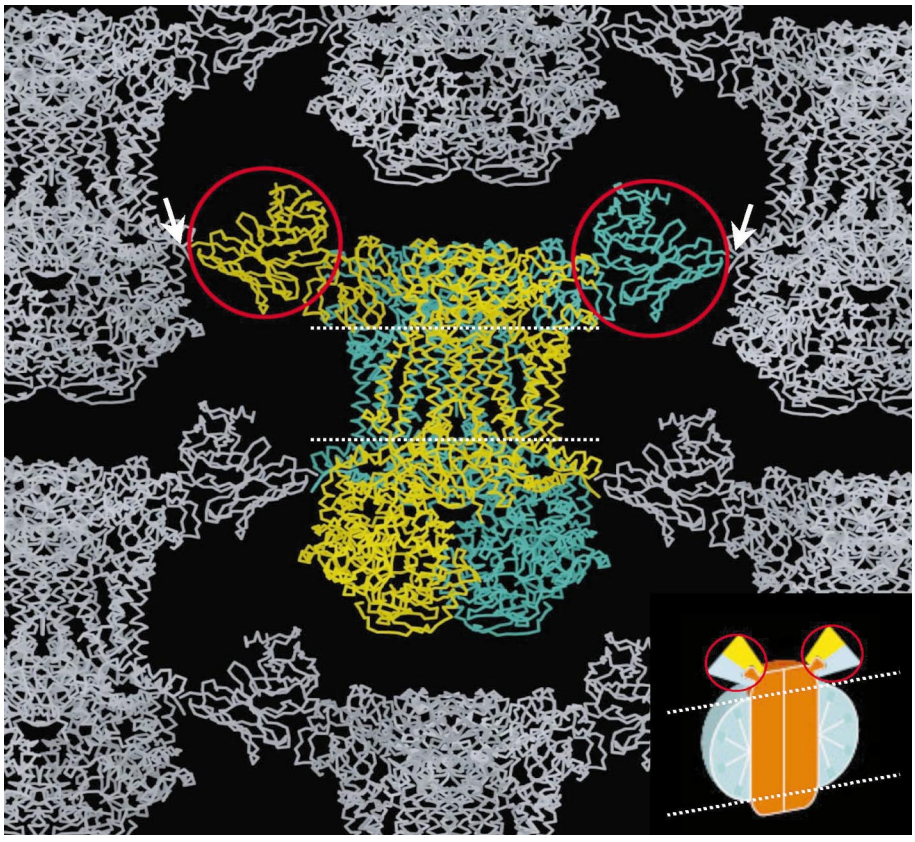

Fig. 2. Essential crystal contacts (white arrows) of the dimeric yeast QCR–Fv fragment complex are mediated by the Fv fragment (encircled in red). The fragment binds to the extrinsic domain of the Rieske protein and generously provides space for the detergent micelle, in which the transmembrane portion of the complex (dotted lines) is embedded, as schematically depicted in the insert. The central molecule of the crystal packing is coloured in green and yellow, the neighbouring molecules in grey.

protein with a Fe_2S_2 iron–sulfur centre, and cytochrome c_1 with a covalently attached haem c group (Fig. 3A,B). The enzyme is a functional dimer, it has two sites for quinol oxidation, for quinone reduction and most likely for cytochrome c binding. Each Q_o site is constructed by the catalytic domains of cytochrome b and cytochrome c_1 of one monomer and the Rieske protein of the second monomer, to which the latter subunit is bound with its transmembrane anchor. Monomerization of the complex would disrupt the integrity of the site of quinol oxidation, the catalytic centre of the complex. Distances and arrangements of the cofactors obviously allow fast electron transfer within a functional unit (Fig. 3C) [5–8]. Whether the catalytic reactions of the two functional units are coordinated or whether they operate independently is a matter of debate [2,5,9,29].

One of the striking features of the first QCR structures was the finding that the extrinsic domain of the Rieske protein is mobile. The domain was not resolved in the first structure [5] and found in different orientations in the second [6]. It seems that the domain has to be fixed either by inhibitor binding or crystal contacts to be seen in a crystal structure. The movement of the Rieske domain facilitates the transfer of the iron–sulfur cluster from a position close to haem b_L to a position close to haem c_1 (Fig. 3C). The resulting orientations of the cofactors are well suited for electron transfer, indicating that the mobile domain shuttles electrons between cytochrome b and cytochrome c_1 [6]. The extrinsic domain is connected with the transmembrane anchor by a flexible linker region. Modifications in the linker region, which shorten, elongate or increase rigidity of the linker, are deleterious for the enzyme activity, supporting the view that the mobility of the extrinsic domain is essential [2,30,31]. In the yeast QCR structure the linker is stretched out in the most extended position, but the initial part of the linker forms a 3_{10}-helix that is stabilized by hydrogen bonds with neighbouring residues of cytochrome b. The linker has to wind up when the extrinsic Rieske domain swings towards cytochrome c_1 [6,7] and it is likely that the first helical turn forms a matrix to direct the coiling of the helix [31]. A steered molecular dynamics simulation has shown that the movement between different positions of the mobile domain found in crystal structures is feasible [32]. Additionally, there is some evidence that the orientation of the domain is related to redox condition as shown by EPR [33]. However, the actual mechanism underlying this functionally important domain movement is still unknown [2].

5. Quinone reduction

Quinone reduction takes place at the Q_i site. The binding mode of the natural substrate coenzyme Q6 in this site was described for the yeast QCR structure [8]. The molecule is bound in a hydrophobic pocket, which is accessible from hydrophobic clefts present at each side of the dimer interface in the transmembrane region. The quinone head group is bound close to haem b_H. Its orientation is stabilized by hydrophobic

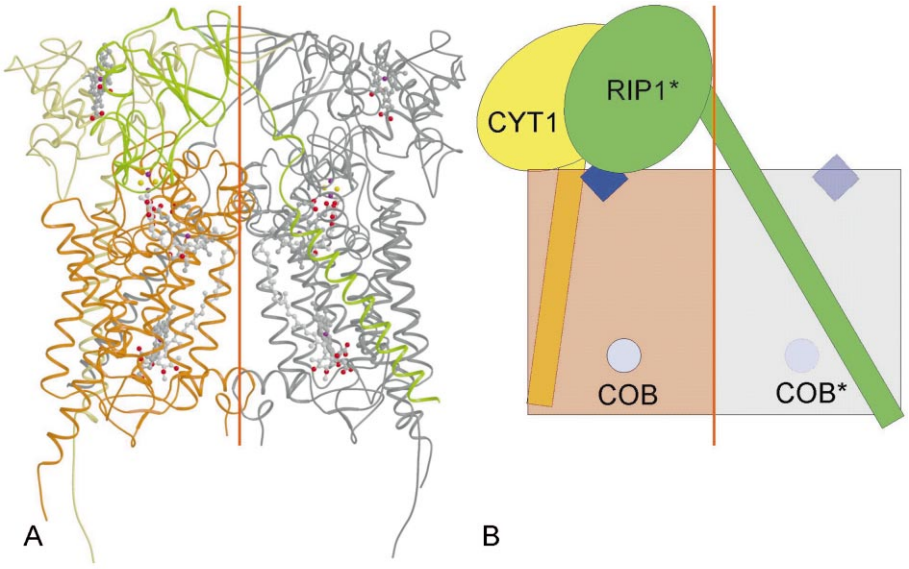

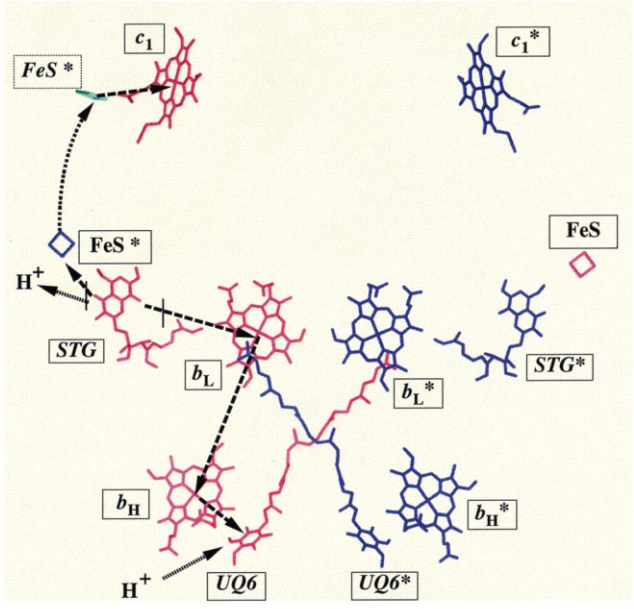

Fig. 3. QCR is a functional dimer. A: Catalytic subunits of yeast QCR. The subunits of one functional unit are colour coded: cytochrome *b*, orange; Rieske protein, green; cytochrome c_1, yellow. The second functional unit is coloured in grey. B: Schematic representation of one functional subunit. The Rieske protein is anchored with its transmembrane helix in one monomer, while the extrinsic domain forms a functional unit with the catalytic subunits of the other monomer. Q_o sites are depicted as diamonds, Q_i sites as circles. C: Orientation of cofactors, substrate and inhibitor molecules in yeast QCR. Monomer A and B are colour coded in red and blue, respectively. The extrinsic domain of the Rieske protein is mobile and the Fe_2–S_2 cluster can be found in different orientations with the maximal positions either close to haem b_L (b-position) or close to haem c_1 (c-position). The latter orientation is found in a bovine QCR structure (X, PDB entry: 1BE3) and the Fe_2–S_2 cluster of the superimposed model is coloured in green. In yeast stigmatellin specifically binds to the Q_o site stabilizing the b-position and inhibiting enzyme activity. Electron transfer and proton uptake are indicated with straight arrows. The curved arrow represents the movement of the Fe_2–S_2 cluster, which most likely precedes oxidation of the cluster by cytochrome c_1. The spatial arrangement of the cofactors allows fast electron transfer.

interactions with Met221 of cytochrome *b* and the bend propionate A of haem b_H (Fig. 4A). Direct and indirect polar interactions are found between side chain atoms of His202, Asp229 and Ser206 of cytochrome *b* and the oxygen atoms of the quinone carbonyl groups (Fig. 4B). Mutational studies have shown that these three residues are critical for enzyme activity [34–36]. However, the oxygen atoms of the quinone carbonyl groups are in closest contact with water molecules, suggesting that these water molecules act as primary proton donors during quinone reduction and protons are consecutively replenished by His202 and Asp229. These residues are connected with the bulk solvent, either directly or by a short array of hydrogen-bonded, buried water molecules [8]. The symmetrical and perpendicular orientation of the quinone ring plane to the plane of the haem porphyrin ring and the existence of two presumable proton donors suggest that the

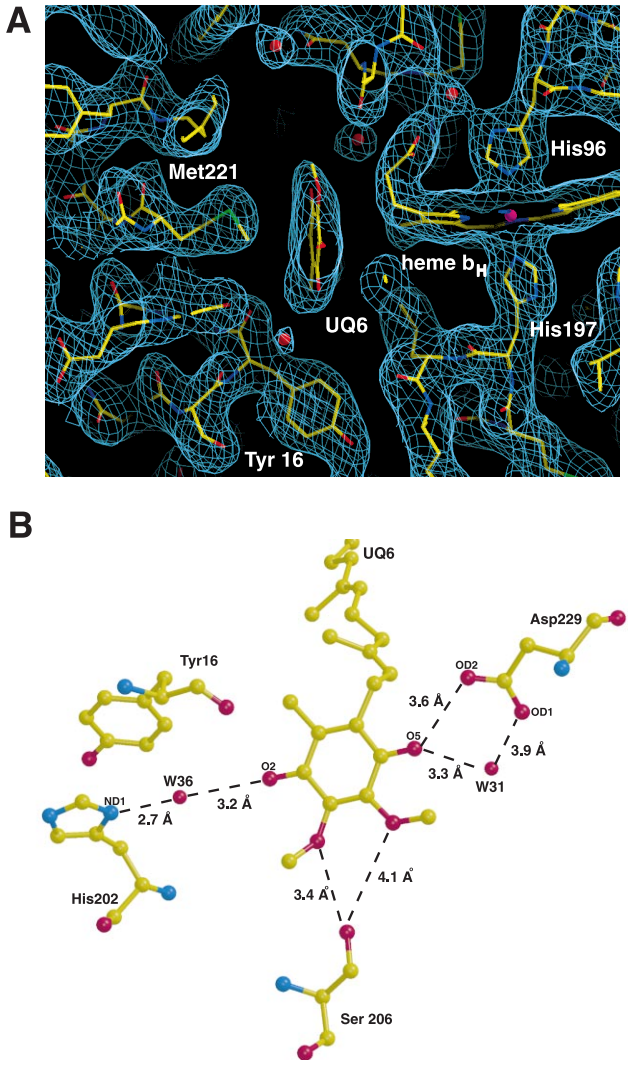

Fig. 4. Binding of the natural substrate coenzyme Q6 (UQ6) at the Q_i site of yeast QCR. A: $2F_o$–F_c electron density map (blue) and refined model close to the high potential haem *b*. Protein model, haem and quinone molecules are shown as stick drawings, water molecules and the haem iron in ball representation. The quinone ring plane is stabilized by hydrophobic interactions with Met221 of cytochrome *b* and by the bend propionate A of haem b_H. B: The orientation of the quinone head group is stabilized by few polar interactions with neighbouring residues. The oxygen atoms of the quinone carbonyl groups are located close to water molecules, suggesting that the latter act as primary proton donors during ubiquinone reduction. Atoms of the relevant amino acid residues and of UQ6 are depicted as ball-and-stick, water molecules as ball presentations.

two-electron and two-proton reduction of quinone can take place without major reorientation of the molecule.

6. Quinol oxidation

The site of quinol oxidation is located close to haem b_L and is formed by cytochrome *b* and the mobile extrinsic domain of the Rieske protein. There is considerable debate whether quinol oxidation requires either one or two quinol molecules bound at the Q_o site, as suggested by the single- [37] or double-occupancy model [38]. Up to now, none of the available native structures showed quinol bound at this site. The Q_o binding pocket is bifurcated and different classes of Q_o site-specific inhibitors are found to occupy two different domains of the pocket [5–9,37,39]. However, this can be interpreted either in favour of or against the double-occupancy model, as the two domains are overlapping. Despite the large number of different spectroscopic and genetic experiments, no conclusive decision in support of one of the models can be taken [2]. Further experiments are required to clarify the important question of Q_o site occupancy.

In the structure of yeast QCR the inhibitor stigmatellin is bound in the Q_o site. Binding of stigmatellin is stabilized by two hydrogen bonds: (1) between the oxygen atom of the carbonyl group of stigmatellin and the ε-nitrogen atom of His181 of the Rieske protein, a ligand of the Fe_2–S_2 cluster, and (2) between the hydroxyl group of stigmatellin and the side chain of Glu272 of cytochrome *b* (Fig. 5). Thereby, the mobile Rieske domain is fixed in the so-called b-position, close to haem b_L. It seems likely that the binding mode of stigmatellin resembles that of a quinol oxidation intermediate as shown for the Q_B site of the reaction centre from *Rhodopseudomonas viridis* [8,40] and that the two residues help to stabilize the enzyme–substrate complex. Mutagenesis of the conserved glutamate results in reduction or loss of quinol oxidation [36], supporting the importance of the residue for the mechanism. The binding of stigmatellin is in agreement with the following basic steps of a quinol oxidation model [2,8,37]. The first electron is transferred to the Fe_2–S_2 cluster, which will be oxidized by haem c_1 after movement of the Rieske domain to the c-position. The second electron reduces haem b_L and two protons are released upon oxidation. It is noteworthy that the binding of the cluster bearing tip of the Rieske protein in the b-position results in a tight interaction of the surfaces of the two interacting subunits, thus excluding access to the bulk solvent [8]. Primary proton acceptors during quinol oxidation are most likely His181 of the Rieske protein and Glu272. The side chain of the latter residue is found in an alternate position in QCR structures with an empty quinol binding pocket [6,7]. It was suggested that the movement of this residue towards an array of buried water molecules connected by hydrogen bonds facilitates a proton exit pathway [8,37]. Suitable water molecules are present in the high-resolution structure of yeast QCR. They are located between the propionate groups of haem b_L and the presumable quinol oxidation site (Fig. 5). Directing the proton towards the haem parallel to the electron transfer might be advantageous for electrostatic reasons, as charge compensation could speed up proton transfer. Release of protons from His181 may take place from the bulk solvent during movement of the Rieske domain to the c-position. There is no consensus about intermediate steps of quinol oxidation. An initial study showed the presence of a transient semiquinone at the Q_o site suggesting a sequential mechanism for the two electron transfer steps [41]. Recent studies demonstrated that a semiquinone radical is not detectable [42], favouring a concerted oxidation of quinol by cytochrome *b* and the Rieske protein [43,44] or a sequential mechanism that includes a rotation of the semiquinone to facilitate rapid oxidation [2,37]. In conclusion, the crucial mechanism of quinol oxidation is still not resolved and its elucidation is a challenge for further studies.

The structures of QCR elucidated important aspects of structure–function relationships in these enzymes. Open questions remain concerning the interaction of the functional units

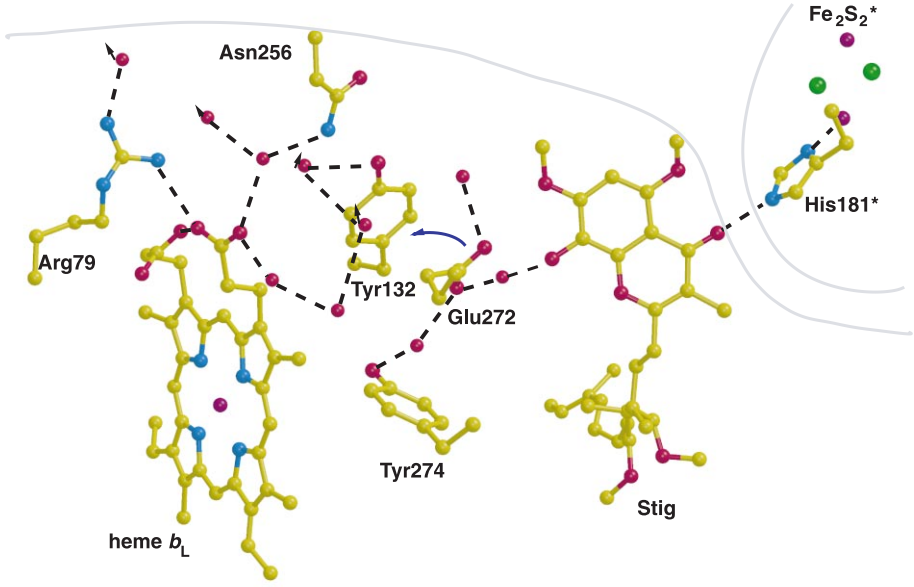

Fig. 5. Binding of the Q_o site-specific inhibitor stigmatellin in yeast QCR resembles the binding of a quinol oxidation intermediate [8]. Hydrogen bonds are present exclusively between the carbonyl oxygen of stigmatellin and His181 of the Rieske protein as well as between the hydroxyl oxygen of stigmatellin and the side chain of Glu272 of cytochrome *b*. An apparent hydrogen-bonding network connects an array of buried water molecules between the Q_o site and haem b_L. Rotation of Glu272 (blue arrow) might open a proton exit pathway during quinol oxidations, which is parallel to electron transfer [8]. Hydrogen bonds are indicated with dotted lines, haem, stigmatellin, and amino acid residues are shown in ball-and-stick representation. Arrows are used to indicate access to the bulk solvent.

within the dimeric molecule, the role of tightly bound phospholipid molecules, and the mechanism of quinol oxidation as well as quinone and cytochrome *c* reduction.

Acknowledgements: The author likes to thank E. Padan and H. Palsdottir for reading the manuscript. The author's work was supported by the DFG (SFB 472) and the Max-Planck-Gesellschaft.

References

[1] Saraste, M. (1999) Science 283, 1488–1493.
[2] Berry, E.A., Guergova-Kuras, M., Huang, L. and Crofts, A.R. (2000) Annu. Rev. Biochem. 69, 1005–1075.
[3] Mitchell, P. (1976) J. Theor. Biol. 62, 327–367.
[4] Brandt, U. and Trumpower, B. (1994) Crit. Rev. Biochem. Mol. Biol. 29, 165–197.
[5] Xia, D., Yu, C.A., Kim, H., Xia, J.Z., Kachurin, A.M., Zhang, L., Yu, L. and Deisenhofer, J. (1997) Science 277, 60–66.
[6] Zhang, Z., Huang, L.-S., Shulmeister, V.M., Chi, Y.-I., Kim, K.-K., Hung, L.-W., Crofts, A.R., Berry, E.A. and Kim, S.-H. (1998) Nature 392, 677–684.
[7] Iwata, S., Lee, J.W., Okada, K., Lee, J.K., Iwata, M., Rasmussen, B., Link, T.A., Ramaswamy, S. and Jap, B.K. (1998) Science 281, 64–71.
[8] Hunte, C., Koepke, J., Lange, C., Rossmanith, T. and Michel, H. (2000) Structure 8, 669–684.
[9] Crofts, A.R. and Berry, E.A. (1998) Curr. Opin. Struct. Biol. 8, 501–509.
[10] Michel, H. (1983) Trends Biochem. Sci. 8, 56–59.
[11] Kuehlbrandt, W. (1988) Q. Rev. Biophys. 21, 429–477.
[12] Garavito, R.M., Picot, D. and Loll, P.J. (1996) J. Bioenerg. Biomembr. 28, 13–27.
[13] Ostermeier, C. and Michel, H. (1997) Curr. Opin. Struct. Biol. 7, 697–701.
[14] Ostermeier, C., Iwata, S., Ludwig, B. and Michel, H. (1995) Nat. Struct. Biol. 2, 842–846.
[15] Iwata, S., Ostermeier, C., Ludwig, B. and Michel, H. (1995) Nature 376, 660–669.
[16] Ostermeier, C., Harrenga, A., Ermler, U. and Michel, H. (1997) Proc. Natl. Acad. Sci. USA 94, 10547–10553.
[17] Kwong, P.D., Wyatt, R., Robinson, J., Sweet, R.W., Sodroski, J. and Hendrickson, W.A. (1998) Nature 393, 648–659.
[18] Padan, E., Venturi, M., Michel, H. and Hunte, C. (1998) FEBS Lett. 441, 53–58.
[19] Venturi, M., Rimon, A., Gerchman, Y., Hunte, C., Padan, E. and Michel, H. (2000) J. Biol. Chem. 275, 4734–4742.
[20] Kleymann, G., Ostermeier, C., Ludwig, B., Skerra, A. and Michel, H. (1995) Bio/Technology 13, 155–160.
[21] Ostermeier, H. and Michel, H. (1996) Nucleic Acids Res. 24, 1979–1980.
[22] Hogenboom, H.R., de Bruine, A.P., Hufton, S.E., Hoet, R.M., Arends, J.-W. and Roovers, R.C. (1998) Immunotechnology 4, 198–216.
[23] Demartis, S., Huber, A., Viti, F., Lozzi, L., Giovanni, L., Neri, P., Winter, G. and Neri, F. (1999) J. Mol. Biol. 286, 617–633.
[24] Hanes, J., Schaffitzel, C., Knappik, A. and Plückthun, A. (2000) Nat. Biotechnol. 18, 1287–1292.
[25] Kim, C.H., Balny, C. and King, T.E. (1987) J. Biol. Chem. 262, 8103–8108.
[26] Braun, H.-P. and Schmitz, U.K. (1995) Trends Biochem. Sci. 20, 171–174.
[27] Deng, K., Zhang, L., Kachurin, A.M., Yu, L., Xia, D., Kim, H., Deisenhofer, J. and Yu, C.-A. (1998) J. Biol. Chem. 273, 20752–20757.
[28] Makarova, K.S. and Grishin, N.V. (1999) Protein Sci. 8, 2537–2540.
[29] Linke, P., Bechmann, G., Gothe, A. and Weiss, H. (1986) Eur. J. Biochem. 158, 615–621.
[30] Tian, H., Yu, L., Mater, M.W. and Yu, C.A. (1998) J. Biol. Chem. 273, 27953–27959.
[31] Nett, J., Hunte, C. and Trumpower, B. (2000) Eur. J. Biochem. 267, 5777–5782.
[32] Izrailev, S., Crofts, A.R., Berry, E.A. and Schulten, K. (1999) Biophys. J. 77, 1753–1768.
[33] Brugna, M., Rodgers, S., Schricker, A., Montoya, G., Kazmeier, M., Nitschke, W. and Sinning, I. (2000) Proc. Natl. Acad. Sci. USA 97, 2069–2074.
[34] Hacker, B., Barquera, B., Crofts, A.R. and Gennis, R.B. (1993) Biochemistry 32, 4403–4410.
[35] Gray, K.A., Dutton, P.L. and Daldal, F. (1994) Biochemistry 33, 723–733.

[36] Brasseur, G., Saribas, A.S. and Daldal, F. (1996) Biochim. Biophys. Acta 1275, 61–69.
[37] Crofts, A.R., Barquera, B., Gennis, R.B., Kuras, R., Guergova-Kuras, M. and Berry, E. (1999) Biochemistry 38, 15807–15826.
[38] Ding, H., Moser, C.C., Robertson, D.E., Tokito, M.K., Daldal, F. and Dutton, P.L. (1995) Biochemistry 34, 15979–15996.
[39] Kim, H., Xia, D., Yu, C.A., Xia, J.Z., Kachurin, A.M., Zhang, L., Yu, L. and Deisenhofer, J. (1998) Proc. Natl. Acad. Sci. USA 95, 8026–8033.
[40] Lancaster, C.R.D. and Michel, H. (1997) Structure 5, 1339–1359.
[41] De Vries, S., Albracht, S.P.J., Berden, J.A. and Slater, E.C. (1981) J. Biol. Chem. 256, 11996–11998.
[42] Jüneman, S., Heathcote, P. and Rich, P.R. (1998) J. Biol. Chem. 273, 21603–21607.
[43] Snyder, C.H., Gutierrez-Cirlos, E.B. and Trumpower, B.L. (2000) J. Biol. Chem. 275, 13535–13541.
[44] Link, T.A. (1997) FEBS Lett. 412, 257–264.